# Lab on a Chip

Accepted Manuscript

This is an *Accepted Manuscript*, which has been through the Royal Society of Chemistry peer review process and has been accepted for publication.

Accepted Manuscripts are published online shortly after acceptance, before technical editing, formatting and proof reading. Using this free service, authors can make their results available to the community, in citable form, before we publish the edited article. We will replace this *Accepted Manuscript* with the edited and formatted *Advance Article* as soon as it is available.

You can find more information about *Accepted Manuscripts* in the **Information for Authors**.

Please note that technical editing may introduce minor changes to the text and/or graphics, which may alter content. The journal's standard **Terms & Conditions** and the **Ethical guidelines** still apply. In no event shall the Royal Society of Chemistry be held responsible for any errors or omissions in this *Accepted Manuscript* or any consequences arising from the use of any information it contains.
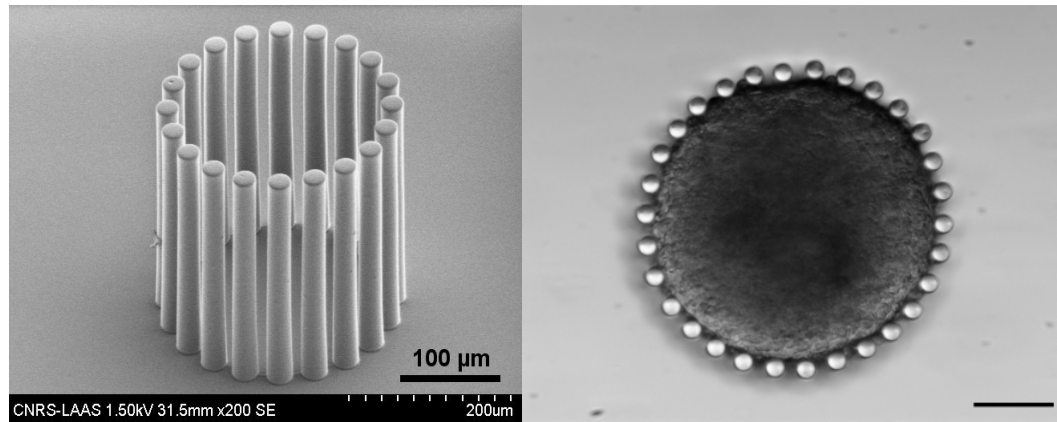
A PDMS microdevice made of a circle of high aspect ratio micro-pillars, acting as flexible force sensors, dedicated to the investigation of mechanical properties at tissue-scale.

Lab on a chip

ARTICLE

Microdevice arrays of high aspect ratio Poly(DiMethylSiloxane) pillars for the investigation of multicellular tumour spheroid mechanical properties.

Laurène Aoun[abcd], Pierre Weiss[cd], Adrian Laborde[ab], Bernard Ducommun[cde], Valérie Lobjois[*cd] and Christophe Vieu[*af]

We report the design, the fabrication and evaluation of an array of microdevices composed of high aspect ratio PDMS pillars, dedicated to the study of tumour spheroid mechanical properties. The principle of the microdevice is to confine a spheroid within a circle of micropillars acting as peripheral flexible force sensors. We present a technological process for fabricating high aspect ratio micropillars (300 μm high) with tunable feature dimensions (diameter and spacing) enabling to produce flexible PDMS pillars, with a height comparable to spheroid sizes. This represents an upscale of 10 along the vertical direction in comparison to more conventional PDMS pillar force sensors devoted to single cell studies, while maintaining their force sensitivity in the same order of magnitude. We present a method for keeping these very high aspect ratio PDMS pillars stable and straight in liquid solution. We demonstrate that microfabricated devices are biocompatible and adapted to long-term spheroid growth. Finally, we show that spheroid interaction with micropillars' surface is dependent on PDMS cellular adhesiveness. Time-lapse recordings of growth-induced micropillars' bending coupled with a software to automatically detect and analyse micropillar displacements are presented. The use of these microdevices as force microsensors opens new perspectives in the fields of tissue mechanics and pharmacological drug screening.

Introduction

A tumour micro-region consists of a 3D heterogeneous cell population in which cancer cell growth is influenced by its interaction with the microenvironment. The crosstalk between tumour cells and microenvironmental components, including the extracellular matrix (ECM), fibroblasts, endothelial and immune cells, is essential for tumour progression and drug resistance[1, 2]. In such a complex environment, tumour growth and progression is influenced not only by biochemical parameters such as growth factors, cytokines, hormones or hypoxia, but also by mechanical cues[3, 4]. Indeed, sensing compression and tension forces (i.e., mechano-sensing) is an important component of cell physiology and changes in mechanical homeostasis within tissues are observed during tumour growth. Several studies have shown that a modification of the mechanical environment can modulate tumour cell growth, migration and invasion as well as proliferation and apoptosis[5-9]. However, little is known about the intrinsic tumour mechanical properties.

MultiCellular Tumor Spheroids (MCTS) are 3D models that accurately reproduce the organization of a micro-tumour, recapitulating cell-cell and cell-microenvironment interactions[10]. Growing spheroids display a proliferation gradient in which proliferating cells are located in the outer cell-layers and quiescent cells are located in the center. This proliferation gradient develops gradually during spheroid growth, right after the establishment of decreasing nutrients and oxygen gradients from the periphery to the centre of the spheroid. This cell proliferation regionalization is similar to what is observed in tumour micro-regions[10, 11]. Given the role played by the mechanical characteristics of cells and tissues in tumour development, a number of studies devoted to the exploration of tissue mechanical properties were performed on spheroids. Different experimental approaches were developed, such as for instance the use of parallel-plate tensiometry or micropipette aspiration to investigate the response of multicellular aggregates subjected to compressive stress. However, if these approaches allow the determination of some relevant physical parameters, they do not give access to the forces exerted by the growing spheroid on its environment[12, 13].

However, if one is interested by the cellular level rather than the multi-cellular or tissue level, several experimental methods have been developed to quantify forces exerted by cells on their environment [14]. Among them, traction force microscopy using a matrix of microfabricated deformable Poly(DiMethylSiloxane) (PDMS) pillars [15-18] has been at the core of intense research. In the majority of the studies devoted to single cell force measurement, the height of the PDMS micropillars does not exceed 100 µm with a maximum aspect ratio, defined here as the ratio between pillar height and pillar diameter, comprised between 6 and 10. The advantage of the method relies on the local control of the pillar stiffness through its geometrical dimensions. From a technological point of view, when we consider the Young modulus of PDMS and the mechanical stability of these pillars, the softest PDMS pillars reported yet exhibited a spring constant around 1 nN/µm, allowing for the measurement of forces in the order of a few nN on single focal adhesion sites[19]. Albeit very attractive, the application of this strategy to spheroids requires the microfabrication of straight and flexible, high PDMS micropillars (around 300 µm high) with aspect ratio around 10. A number of papers have described the fabrication of high aspect ratio PDMS pillars either for investigating their mechanical stability or for nanoNewton force measurements[20-22]. All these reports point out the mechanical instability of PDMS pillars exhibiting aspect ratios of 5-10. In our work we also witness the collapse of the high aspect ratio PDMS structures after demolding, making them really challenging to produce and to employ for tissue scale biological applications[23, 24]. Indeed, it can be easily shown that, as the spring constant of a cylindrical PDMS pillar is proportional to d^4/L^3, (where d is the pillar diameter and L its height), upscaling the PDMS force sensor in the z direction (increasing its height L) with a factor α while keeping its force sensitivity constant (same spring constant), requires to increase the aspect ratio of the produced PDMS structure by a factor $\alpha^{1/4}$. Typically, in the present investigation, scaling-up PDMS pillar technology from single cell investigations to spheroid investigations represents a α factor of 100 which requires improvement of the aspect ratio of the produced PDMS pillars by a factor greater than 3.

In this study, we present the design and production of dedicated microfabricated PDMS structures with sizes adapted to tissue scale studies, which enables the characterization of the mechanical interaction of a growing spheroid with its environment. The principle of the microfabricated devices is to confine the spheroid inside a cavity of a fixed volume equipped with a corral of PDMS high aspect ratio pillars acting as force sensors at its periphery. Through an optimization of the fabrication process and a dedicated method to straighten collapsed PDMS pillars, we show that the microfabricated devices are adapted and compatible with MCTS growth over time and that the high aspect ratio micropillars are flexible enough to be bent by growing spheroids. Moreover, we have introduced by design, systematic variations of micropillar diameter and spacing in order to generate tunable mechanical constraints to growing tumour spheroids. These devices open the route of cell force measurement at the tissue scale as well as new perspectives in the fields of tumour multicellular model mechanics and pharmacological drug screening.

Materials and methods

Design of the microdevices

Each microdevice is an arrangement of 300 µm high cylindrical PDMS micropillars of identical diameter and spacing, circularly distributed around an area where the spheroid will be positioned. Each produced PDMS chip contains an array of microdevices sets exhibiting some dimensional variations in pillar diameter (30, 35, 40 up to 72 µm), spacing between pillars (5, 10, 20, 30 µm) and overall diameter of the device (200 to 350 µm). One set of microdevices is constituted of 8 units, allowing to multiply at once the number of experiments for a given sample or condition (Fig. 1). For example 4 sets of microdevices accommodates a 1 cm² PDMS chip that contains 32 microdevices. Each set is identified by an imprinted code of numbers and a letter that allows identification of the corresponding geometrical dimensions. These PDMS chips are obtained by casting a PDMS pre-polymer solution on a microfabricated master mould and solidifying the polymer by thermal curing before unmoulding.
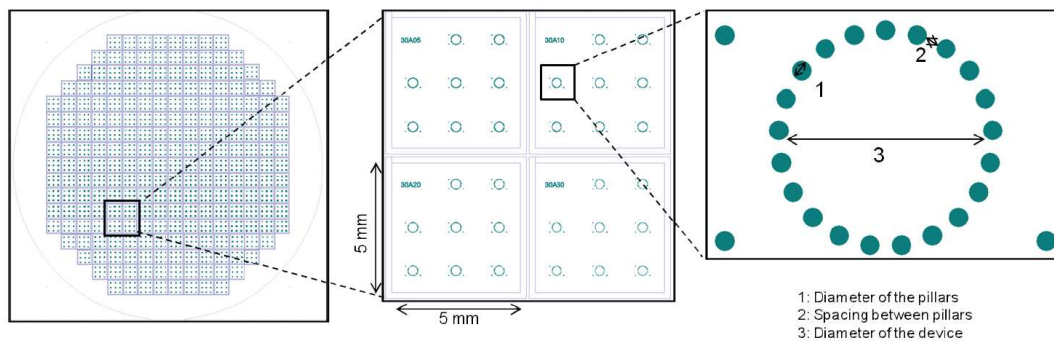

Fig 1. Technological design of the arrays of mirodevices. Left: sketch of the 4 inches SU8 mold containing arrays of microdevices. Middle: 1 cm² chip contains four sets of eight microdevices. Right: Each microdevice exhibits a circle of equidistant pillars and three reference pillars outside of the corral. Each set corresponds to a given combination of three morphological parameters: the diameter of the pillars, the spacing between the pillars, and the diameter of the circle.

Lab on a chip

ARTICLE

Fabrication of the master mould

The master mould used for this work was made of a thick photoresist layer microstructured by optical lithography on a 4 inches silicon wafer. We have optimized the photolithography and development process on a SU-8 3000 (MicroChem Inc.) epoxy-type, near-UV negative photoresist, in order to obtain high aspect ratio cavities. The lithography process involved two steps. First, a 10 μm thick layer of SU-8 3005 photoresist was spin coated onto a silicon wafer, soft baked, followed by UV flood exposure for 7 s and postbaked. This bottom layer was used to insure the attachment of the second resist layer to the wafer. A second layer of SU-8 3050 with a thickness of 300 μm was spin coated in two steps, directly on top of the first layer and soft baked overnight at 95°C. The wafer was then placed in vacuum contact with the chromium/glass optical mask that contained the desired patterns and exposed to UV light using a UV filter (λ=365 nm), in a Suss Microtec MA6 Optical aligner. The wafer was postbaked and developed in PGMEA (propylene glycol methyl ether acetate) under agitation and primary vacuum for 2 hours. Once the development of the cavities was completed, the wafer was washed with isopropyl alcohol and hard baked. The surface of the SU-8 mould was treated with a octadecyltrichlorosilane (OTS) in liquid phase before PDMS replica moulding. On a 4 inches wafer, 1024 microdevices are generated displaying 128 different combinations of the varied geometrical dimensions (more details on the fabrication process are given as supplementary data).

Production of PDMS microdevices

PDMS replicas were fabricated as follows. PDMS pre-polymer (Sylgard 184®) was mixed with the reticular agent at a 10:1 ratio, poured on the 4 inches SU-8 master mould, degassed for a few minutes and cured at 80°C for at least 5 hours. A small chip of PDMS of 4 cm^2, suitable for biological investigations, was then carefully cut with a razor blade directly on top of the wafer and this small piece of PDMS was gently unmoulded. Special attention has been paid to unmould each PDMS chip after curing in order to avoid the possible collapse of the high aspect ratio PDMS pillars. Some chips were unmoulded conventionally in air with the risk of collapse of the PDMS pillars of small diameter (30 μm) and other chips were unmoulded in ethanol and dried in a CO_2 critical point dryer machine (Automegasamdri-915B, Series C, Tousimis®). PDMS pillars were morphologically characterized by Scanning Electron Microscopy, in order to measure their height, shape, diameter and spacing. As cell culture occurs in liquid medium,

the injection of a liquid solution on the PDMS chips may cause damage of the microdevices, by inducing some pillar collapse when the liquid front invades the surface. In order to investigate these effects, different solutions were tested: Di water, culture medium (DMEM-Dulbecco's Modified Eagle's Medium), PBS (Phosphate Buffered Saline) and PBS with 5% BSA (Bovine Serum Albumin), with the intention to see if these mechanical effects on the PDMS pillars were solution dependent or not. In these experiments, the PDMS chips were placed directly into a petri dish prior addition of the liquid solution. Upon liquid injection, it was observed that an air bubble was systematically trapped at the centre of each circular device. These bubbles were delicately removed one by one by a simple microtweezer movement under optical inspection.

Cell culture, spheroids generation and manipulation

HCT116 colon cancer cells (ATCC) were cultured in DMEM medium, supplemented with 10% foetal calf serum FCS (Invitrogen, France) and 1% penicillin/streptomycin in a humidified atmosphere of 5% CO_2 at 37°C. Spheroids were prepared in the same medium from $5x10^2$ cells in 100 μL loaded in each well of a poly-HEMA coated 96-well plates. The plates were centrifuged at 600 g for 6 min and then incubated in a humidified atmosphere of 5% CO_2 at 37°C. After 3 days, spheroids of about 300μm in diameter were recovered from each well and transferred one by one to a PDMS microdevice either by direct micropipeting or by lifting them gently with a microtweezer (Fig. 5).

Images acquisition

Time-lapse videomicroscopy experiments were carried out for at least 30 hours (1 frame/10 min), using an inverted wide field Zeiss Axio Observer Z1 microscope fitted with a 0.3 N.A 10X objective, at a temporal frequency of 1 frame/10 min. For confocal experiments, prior to the positioning of the spheroid inside the microdevices, pillars were stained with the lipophilic tracer DiI (1,1'-Dioctadecyl-3,3,3',3'-Tetramethylindocarbocyanine Per-chlorate) or DiO (3,3'-Dilinoleyloxacarbocyanine Perchlorate), (both from Invitrogen) at a concentration of 50 μg/ml for 20 min at room temperature, then washed with deionized water and PBS to remove excess staining. Time lapse acquisition were performed at 1 frame/10-20 min using a laser scanning microscope, Zeiss LSM 510 NLO fitted with a water immersion 20X objective.
For experiments running over 5 days, images were taken every 24 hours using a Macrofluo straight microscope (Leica) with a 10X magnification objective.

Image processing and analysis

Pillar tracking and measurements of their lateral displacement were performed using a homemade image processing software developed on MATLAB®. The overall principle of the algorithm is described below.

Pillars are first segmented on each image of the sequence separately. In a given experiment, pillars shapes and radii are constant. This step can thus be achieved by computing a cross-correlation between the image of a disk of fixed radius R and the optical microscopy images. The extreme of the correlation image is then extracted with a greedy algorithm: the first pillar centre is placed at the pixel where the correlation is maximal. All pixels of the correlation image at a distance less than 2R of the pillar centre are then set to 0. The same principle is repeated until all pillars are segmented (i.e. until a given number of pillars is reached). This simple algorithm ensures that the right number of pillars is detected and that the segmented pillars do not overlap. This algorithm works nearly perfectly in the early stages of the spheroid growth. In later stages, the algorithm may fail since the pillars' top can hardly be distinguished from the background. The user can then refine the pillars' location manually with a dedicated graphical interface.

The segmented pillars are then registered rigidly. This step is necessary whenever the acquisition parameters are changed during the spheroid growth. The parameters of the rigid transformation are computed using 3 reference pillars placed outside the circle of pillars, so that they do not move by interacting with the spheroid.

Once all pillars are segmented and registered, the algorithm finds pairings between pillars in consecutive images of the sequence. This step is achieved by using tools from optimal transport. The pairings are chosen in order to minimize an energy computed as the sum of square distances between consecutive centres. This is in some sense the most likely displacement between two consecutive images since it is the one minimizing the elastic energy. The optimal pairing is found by using the so-called Hungarian algorithm[25]. Overall, this simple pipeline provides accurate results with reasonable computing times.

Statistical analysis

Pillar coordinates' data collected from time-lapse experiments were processed using Prism software (GraphPad) through smoothed curves of frequency distribution histograms. We considered the sum of pillars displacement over 5 days.

Results and discussion

Master mould fabrication and PDMS moulded pillars.

Characterization of the SU8 master mould was carried out using Scanning Electron Microscope (SEM) and optical profilometer. SEM images of the fabricated mould (Fig. 2) demonstrate that high aspect ratio cylindrical holes, 300 µm deep with straight and uniform walls, were successfully obtained by our fabrication method, for all micropillars diameters (30-72 µm) and spacing between micropillars (5-30µm).
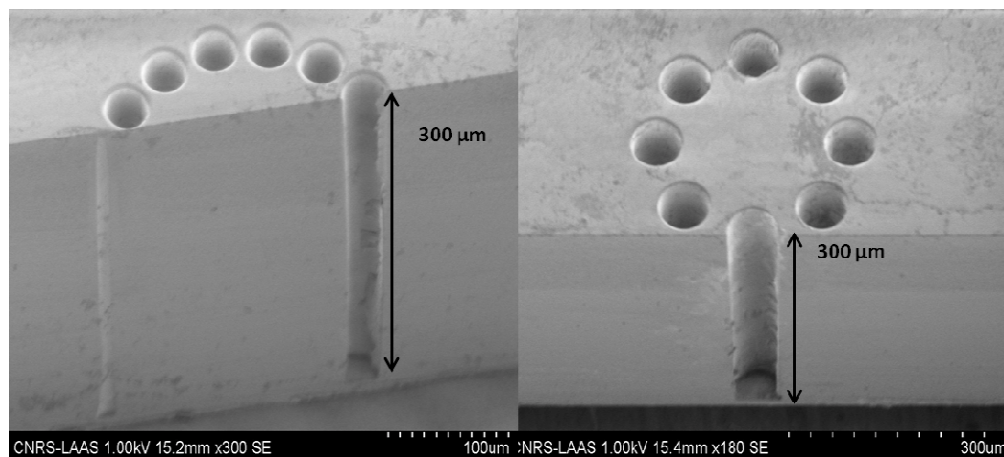

Fig 2. SEM images (tilted views) of 300 µm deep cylindrical cavities (left: 35 µm diameter and right: 55 µm diameter) in SU8 photoresist. The cross section confirms the good definition of the inner cavity form the top to the bottom of the film.

Vacuum contact of the mask turned out to be a key parameter to generate high-resolution transfer with well-defined shape. The exposure time had to be optimized for enabling cross-linking of the whole resist thickness without degrading the lateral resolution of the process. The optimization of the development step was also crucial. Indeed, it is essential to minimize the stress in the photoresist layer, but also to keep the development time long enough to open all the cavities. To address this issue, the access and regeneration of the developer inside the very deep and narrow cavities, corresponding to the PDMS pillars, needed to be assisted. To this aim, we performed the development of the wafer in a vacuum chamber under constant

agitation. Completion of the development process included 3 to 4 cycles of 30 minutes each, during which the wafer was developed then rinsed with isopropyl alcohol to renew the solution. Pillars of 300 µm high and 5µm spacing were especially challenging because small variations could cause the fusion between adjacent cavities. Examples of PDMS microdevices exhibiting cylindrical high aspect ratios pillars can be seen in figure 3. The radius of the pillars is slightly lower at the top but this variation does not exceed 5%, attesting that the circular surface irradiation of the photoresist was correctly transferred along 300 µm due to a large depth of focus and an efficient multi-step development process. This small tapering effect revealed the performance of our technological process with respect to the aspect ratio of the produced structures as large as 10.
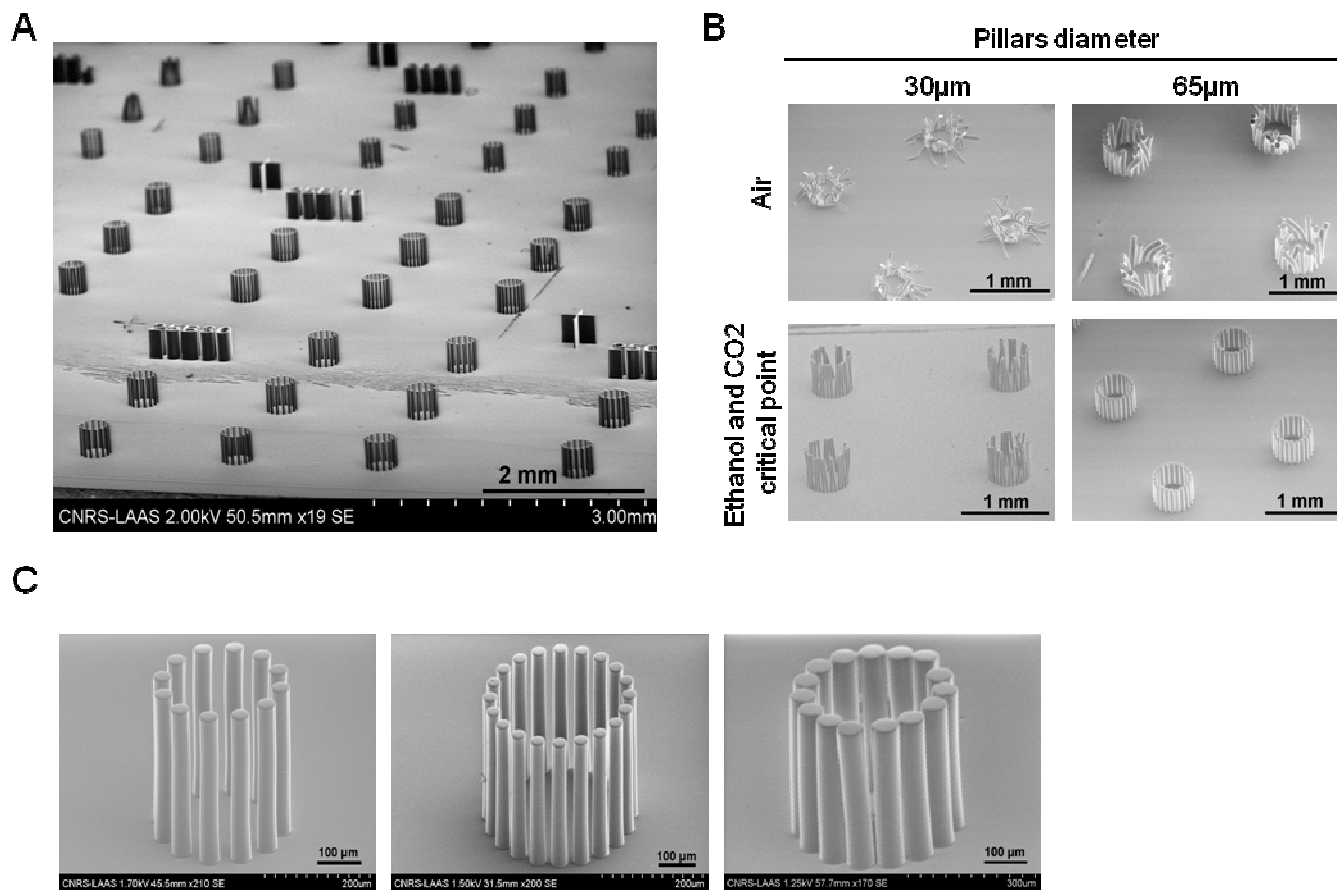

Fig 3. SEM images (tilted views) of a PDMS replica. **(A)** Arrays of PDMS microdevices, all of 300 µm in height. **(B)** High aspect ratio PDMS micropillars either collapsed after unmolding in air for devices with pillars of 30 and 65µm in diameter (top) or remained straight after unmolding in ethanol and drying in a CO_2 critical point dryer machine (bottom). **(C)** Three different straight standing PDMS microdevices (left: pillar diameter 35 µm, pillar separation 20 µm, device diameter 200 µm; middle: pillar diameter 30 µm, pillar separation 10 µm, device diameter 300 µm; right: pillar diameter 60 µm, pillar separation 5 µm, device diameter 250 µm).

Tuning pillar collapse by liquid immersion and surface treatment

For the thinner pillars (30 µm in diameter), collapse of the PDMS structures was observed due to the very poor stiffness of these high aspect ratio (10) polymer features, subjected to various surface forces, such as adhesive forces that lead to lateral and ground collapse[26]. The mechanical collapse of the structures was observed right after the unmoulding process when performed directly in air (Fig. 3B). Since the use of this kind of device relies on the observation of the bending of the PDMS beams when confronted to cell forces, it was of major importance to avoid the collapse of the structures. The diameter of the pillar could not be increased, because this renders the beam stiffer and decreases the sensitivity of the force sensor. To solve this issue we therefore explored two strategies: i) either avoid the collapse during the unmoulding step or ii) find a solution for lifting up the pillars after their collapse. To

implement the first strategy, we unmoulded each PDMS chip in ethanol solution then transferred the chip under ethanol in a CO_2 critical point dryer system in order to avoid any surface tension effects during the drying of the PDMS surface. This resulted in straight standing pillars both for small (30μm) and large (65μm) diameters (Fig. 3B). SEM characterization confirmed the achievement of microdevices with the expected micropillar diameters both for small and large diameters and spacing between pillars (Figure 3C). However, spheroids culture requires the immersion of the devices in biological aqueous solutions. To that purpose, we investigated the second strategy called "reversible collapse" that relies on immersing the PDMS chip, after unmoulding in air, inside a liquid solution in order to straighten the collapsed PDMS beams. The idea was to tune capillary forces during the process in order to recover their straight position. As explained in the materials and methods section, whichever the liquid solution under investigation is, we observed that an air bubble was trapped at the centre of each PDMS pillars' corral after liquid immersion. For practical use of these devices it was therefore necessary to remove these bubbles using the tip of a microtweezer. It turned out that during the escape of the air bubble, in certain conditions, the capillary forces exerted on the collapsed PDMS pillars around the bubble resulted in their straightening. When the devices were covered with deionized water or PBS, the pillars of small (30 μm) as well as large diameters (65 μm) were not standing straight after air bubble removal (Fig. 4 up panel) and not exploitable for any further experiments. In these experimental conditions, capillary forces do not induce the straightening of the pillars. However, as immersion capillary forces depend on surface energy, we have investigated in details the influence of the hydrophilicity of the PDMS chip as well as the nature of the liquid medium. Immersion of the devices in the culture medium of the HCT116 spheroids, with foetal calf serum (FCS) containing proteins (DMEM/10%FCS) turned out to induce a straightening of the pillars after air bubble removal (Fig. 4 bottom panel left column). As the main difference between water or PBS and this culture medium is the presence of proteins inside the solution, we tested the influence of the addition of proteins (Bovine Serum Albumine, (BSA)) in PBS. As shown in Figure 4 (bottom panel central column), in this saline buffer solution enriched with proteins, the PDMS pillars are straight after air bubble removal.
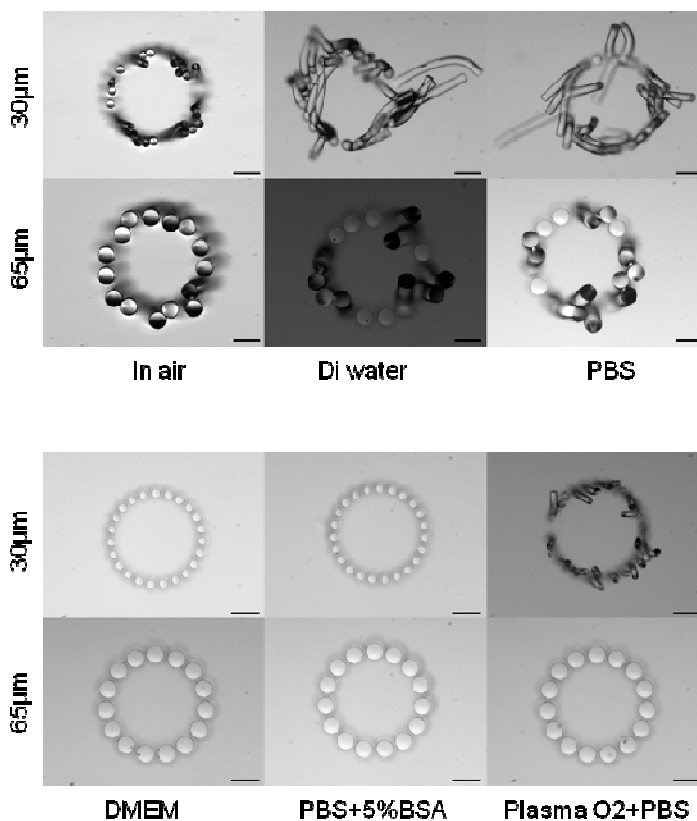

Fig 4. Aspect (transmitted light optical microscopy images) of the PDMS microdevices unmolded in air and immersed in various liquid solutions for pillars of 30 and 65 μm in diameter. Pillars appear collapsed after immersion with deionized water and phosphate buffer solution (PBS) (top panel) but stand straight after immersion with culture medium (DMEM), PBS with 5% BSA and after plasma O_2 treatment. Scale bar: 100μm.

From these experiments, we concluded that the adsorption of proteins at the PDMS surface, which is already reported in the literature[27], was responsible for the raising of the collapsed structures. In some reports, BSA coupled to a fluorescent marker was used to visualize the pillars, showing that BSA adsorbs efficiently to PDMS pillars[28]. Native PDMS, just after unmoulding, is very hydrophobic with a typical contact angle of 110°, but it changes to hydrophilic upon protein coating. To confirm that pillars' straightening is dependent on surface energy, PDMS microdevices were exposed to a O_2 plasma treatment at 200W for 1 min, a duration that is sufficient to render its surface hydrophilic with a typical contact angle of 24°[29]. As shown in Figure 4, collapsed pillars, when immersed in PBS after O_2 plasma treatment, also display a tendency to stand right. Notice that the raising of 30 µm pillars in PBS after O_2 plasma treatment is incomplete, but in this case a damage of the pillars after plasma treatment cannot be completely ruled out. We also immersed O_2 plasma treated PDMS devices in PBS enriched with 5% BSA and the results were similar as with PBS alone (data not shown). All together, these observations led us to conclude that reversible collapse of the high aspect ratio PDMS pillars could be obtained by immersing the PDMS chips in a liquid solution as long as their surface energy had been changed either by plasma treatment or even more efficiently through protein adsorption. The interpretation of this phenomenon may be understood by looking at the orientation of the capillary forces occurring at the meniscus of an air bubble trapped between collapsed PDMS pillars and released by mechanical action. On hydrophilic pillars, the liquid bridge formed below the released bubble, exerts a capillary force that tends to attract the pillars lying around the bubble towards the centre of the device and lift them up. On the contrary, on hydrophobic pillars, the liquid bridge invading the space below the released bubble does not induce any straightening of the pillars due to a repulsive capillary force between the pillars around the bubble. Of course, this rough picture does not take into account in detail all the multiple mechanical interactions between all the pillars placed in circle around the air bubble, but gives a general scheme for understanding the observed effects. In any case, we would like to point out that the origin of these effects comes for the trapping of an air bubble in a site where PDMS pillars are symmetrically distributed. More investigations would be necessary to learn more about this reversible collapse under liquid immersion and investigating its real robustness for different arrangement of flexible structures on the surface.

In conclusion, we propose a very efficient method for using the PDMS chips in a biological solution while maintaining the high aspect ratio PDMS pillars straight and flexible. We simply unmould the PDMS chips in air, then we operate a straightening of the beams with a simple immersion in the protein rich culture medium and by removing the air bubble trapped on each device. This process was used for the rest of the experiments discussed in this paper. After the optimization steps of this process and during the development of our research, we have fabricated 4 SU-8 molds and more than 150 PDMS replicas, with the pillar dimensions specified in this paper. All final PDMS devices turned out to be functional for biological experiments attesting for a very high success rate. The softest produced PDMS pillars (30 µm diameter, 300 µm high) exhibit a spring constant of approximately 13 nN/µm, which is comparable to those reported for single cell investigations. In other words, we have successfully up-scaled by two orders of magnitude the height of the PDMS force sensors without damaging their force sensitivity, thus enabling the investigation of mechanical properties of very large assemblies of cells.

Growth of spheroids within PDMS microdevices.

As shown in Figure 1, various microdevices were fabricated with different diameters in order to allow the investigation of spheroids of various sizes. Pillars of different stiffnesses were produced to measure various ranges of cell forces generated by distinct cell lines, which may have different mechanical properties. These arrays of different microdevices thus turned out to be well adapted to analyse the impact of micropillar rings on spheroid culture and to characterize the displacement of the PDMS pillars in contact with the spheroids. As a biological validation of these microdevices, we analysed by time-lapse experiments the growth of HCT116 spheroids placed at the centre of the microdevices (Fig. 5, supplementary movie 1). In agreement to the above reported results, PDMS microdevices were unmoulded in air and placed in petri dishes containing complete culture media. Spheroids measuring approximately 300µm in diameter were transferred into microdevices of same diameter using a micropipette, and then petri dishes were placed on the stage of an inverted microscope. In parallel experiments, spheroids were grown within the microdevices for durations exceeding one week. We did not observe any sign of toxicity over a long period of time thus confirming the biocompatibility of our PDMS chips with long-term cell culture.

Upon growth of the spheroid within the microdevice, cells progressively get in contact with the PDMS pillars. Strikingly, this contact was accompanied by a modification of cell organisation at the spheroid surface with ruffling and protuberance of group of cells attempting to infiltrate between the pillars (Fig.6, supplementary movie 1). After several days of growth within the microdevice, the spheroid totally embraced the microdevice. Indeed, micropillars 3D patterns were visible when the spheroid was removed from the microdevice (Fig. 6B), showing that the whole spheroid organization was not disrupted. Spheroids turned out to to be reactive to the mechanical and geometrical constraints imposed by the ring of PDMS pillars, but the cohesion of the cells inside the spheroid was not disrupted by this stimulus.
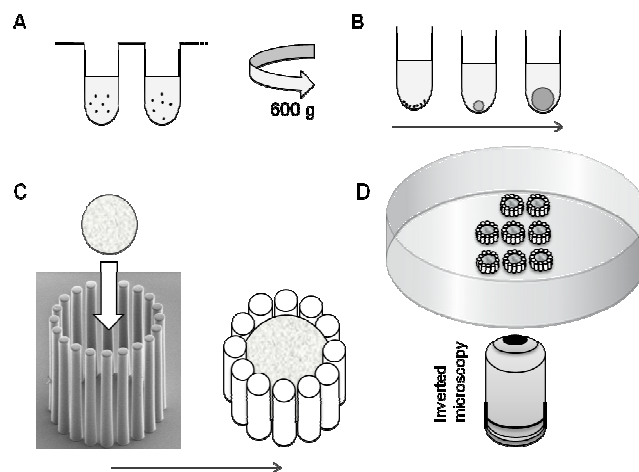
Lab on a chip

ARTICLE

Fig 5. Schematic representation of the production of spheroids and experimental setup. **(A)** Cells were seeded on low adherent well plates then centrifuged at 600g for 6 minutes. **(B)** Cells aggregated and compacted to form a growing spheroid in each well. **(C)** When spheroids reached 300μm in diameter, they were transferred into microdevices placed in a petri dish, using a micropipette. **(D)** The petri dish containing the devices with the spheroids was placed in a videomicroscope for time-lapse observation of the array of devices (Final drawing not at real scale).
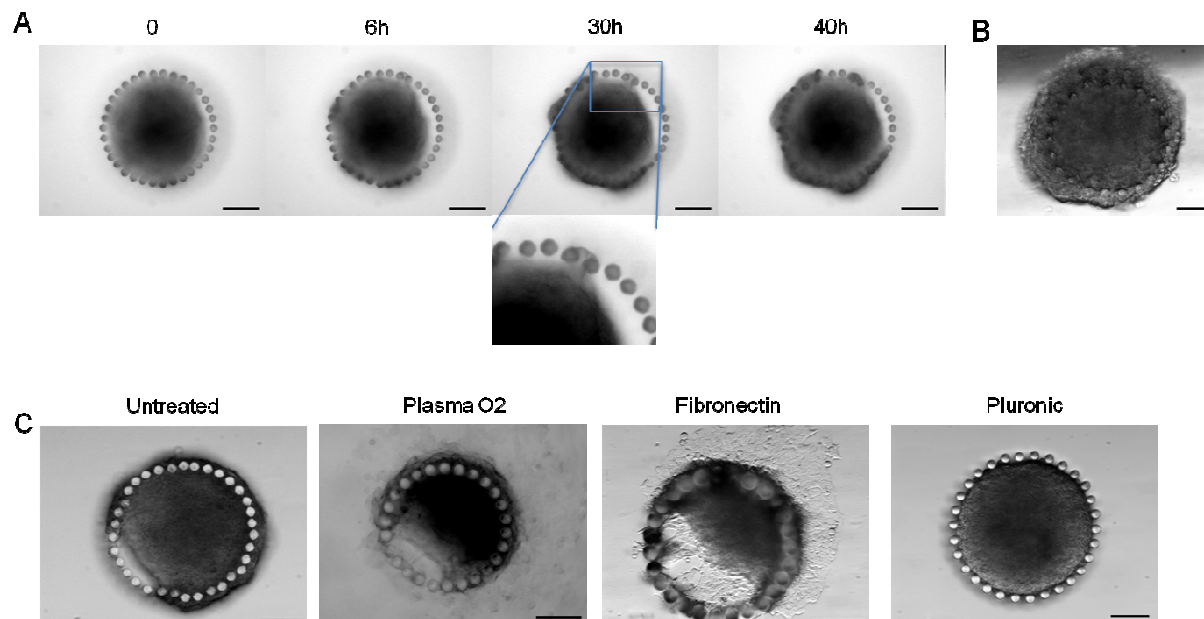

Fig 6. (A) Transmitted light images of a HCT116 spheroid at the time of placement inside the device (t=0h), and after 6h, 30h and 40h of time-lapse imaging under growing conditions. At 30h, protuberance of a group of cells attempting to infiltrate between the pillars is shown in the enlarged view. The device used is constituted of pillars of 30μm in diameter spaced by 5μm. **(B)** The spheroid is removed from the device after 55h and observed from the bottom. Clear imprints left by the pillars are visible. **(C)** The images show spheroids after 24 h grown in an untreated PDMS device, in a O₂ plasma treated PDMS device, in a fibronectin coated PDMS device or in a PDMS device treated with Pluronic-F127. Scale bar: 100μm.

Lab on a chip   RSC**Publishing**

ARTICLE

Spheroids interaction with micropillars' surface is dependent on cell adhesion on PDMS surfaces.

The 3D patterned spheroids were not damaged upon removal from the microdevices suggesting that cells did not adhere strongly on the PDMS surface. To test this hypothesis, we first performed surface treatment to modify the adhesiveness of PDMS pillars to learn about the resulting effect on spheroid behaviour. PDMS is intrinsically a hydrophobic surface that can be oxidized by O_2 plasma treatment. This treatment has been known to turn PDMS surface into hydrophilic and to favour cell adhesion[30]. In order to increase cell adhesion we also coated PDMS with fibronectin, a glycoprotein of the extracellular matrix that binds to plasma membrane-spanning integrins. In both conditions, cell adhesion occurred on the surface inducing migration, and the spheroid organization was progressively disrupted (Fig. 6C). On the contrary, to suppress cell adhesion to PDMS surface, we used Pluronic-F127 treatment, that reduces protein adsorption on PDMS surface[28, 31, 32]. In that condition, no cell interaction with the PDMS surface was visible and cells did not evade from the spheroid (Fig. 6C). These results showed that in the untreated condition, cells slightly interact with PDMS surface through mechanisms that are distinct from cell adhesion and migration machinery.

Growth of spheroids within microdevices induces pillar displacements.

Confocal time-lapse experiments were performed using PDMS micropillars stained with a fluorescent dye. As shown in supplementary movie 2, we observed a displacement of the micropillars, suggesting that this could result from a mechanical action exerted by a group of cells toward the pillars. To get a better insight into the analysis of this phenomenon, we quantified pillar displacement by measuring the length of the displacement vector at the top of each pillar between two time points on widefield microscopy experiments (Fig. 7). Quantification and analysis of frequency distribution of displacements for pillars measuring 30, 35 or 40µm in diameter showed that stiffer pillars were modestly displaced by the spheroid's cells while, large displacements were observed with softer ones. Control experiments performed in the absence of spheroid showed that the microdevice was stable mechanically under cell culture condition and that displacement of pillars was very limited in amplitude (Fig. 1, Sup data). Altogether, these observations strongly suggest that upon contact of the spheroid with the pillars, cells collectively generate forces that can induce pillar displacement and validate the further use of these microdevices for quantifying these forces.

Conclusion

In this study, we have upscaled the PDMS pillar technology in the vertical direction for enabling the investigation of cell forces at a multicellular scale. We have proposed a process for obtaining flexible 300 µm high PDMS pillars with a spring constant around 13 nN/µm (as estimated by the classical linear elasticity theory of a bending beam, using a young modulus of PDMS material of 2.8 MPa experimentally measured by us using a macroscopic compression test). This represents an upscale of 10 in the z direction with respect to devices devoted to single cell studies, without any detrimental impact on force sensitivity. An elegant method for generating high aspect ratio PDMS pillars stable and straight in liquid solution has been proposed. It relies on the reversible collapse of the pillars by simple liquid immersion and air bubble removal that takes profit of the capillary forces to straighten the possible collapsed PDMS pillars. We have used these microdevices to evaluate the consequence of multicellular spheroid confinement. We show that growing spheroids are able to generate pillar displacement which could be used as force sensors. The response of growing spheroids to mechanically interacting pillars is dependent on cell adhesion. Interestingly, we demonstrated that under non-adhesive conditions, forces are exerted by growing spheroids and may be sensed by our flexible high aspect ratio pillars. The quantification of the forces exerted by growing spheroids are yet to be studied. This requires an exact determination of the site where the force is applied by the growing spheroid on each pillar, which needs 3D imaging of the interface between the pillars and the spheroid.

The technological approach presented in this work together with the software developed to perform pillar displacement quantification open new and original perspectives for pharmacological drug screening. From the physics field perspective, this work established a proof-of-principle for the use of micropillars arrays as mechanical sensors to monitor the mechanical properties of growing spheroids as well as other developing tissues.
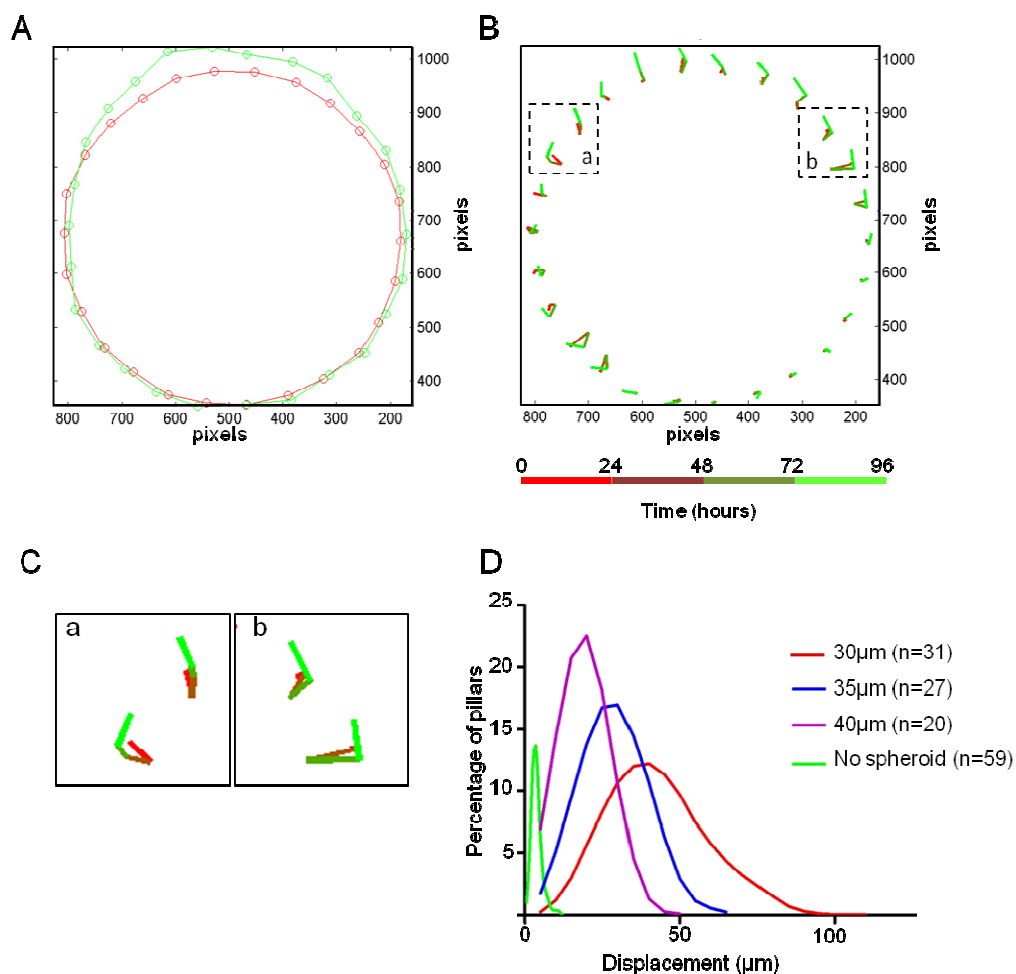
Lab on a Chip Accepted Manuscript

Fig 7. (A) Pillars positions just after spheroid placement at t=0h (in red) and after four days of spheroid growth inside the device (in green). **(B)** Top pillar tracking during 96 hours of experiment. **(C)** Detailed view of some pillars tracks located in the a and b windows pointed in B. **(D)** Histogram of the top pillar displacement induced by spheroid growth for three different pillars diameters. The number of spheroids in each condition is indicated in brackets. In the control condition (no spheroids), the data from devices with the three different diameters have been pooled.

Notes and references

[a] CNRS, LAAS, 7 avenue du colonel Roche, F-31400 Toulouse, France
[b] Univ de Toulouse, LAAS, F-31400 Toulouse, France
[c] CNRS; ITAV-USR3505, Toulouse, France
[d] Univ de Toulouse; ITAV-USR3505, Toulouse, France
[e] CHU de Toulouse; Toulouse, France
[f] Univ de Toulouse, INSA, LAAS, F-31400 Toulouse, France

*To whom correspondence should be adressed. Email: valerie.lobjois@itav-recherche.fr, cvieu@laas.fr.

References

1. A. L. Correia and M. J. Bissell, *Drug Resist Updat*, 2012, **15**, 39-49.
2. D. Hanahan and R. A. Weinberg, *Cell*, 2011, **144**, 646-674.
3. D. T. Butcher, T. Alliston and V. M. Weaver, *Nat Rev Cancer*, 2009, **9**, 108-122.
4. D. Wirtz, K. Konstantopoulos and P. C. Searson, *Nat Rev Cancer*, 2011, **11**, 512-522.
5. G. Cheng, J. Tse, R. K. Jain and L. L. Munn, *PLoS One*, 2009, **4**, e4632.
6. G. Helmlinger, P. A. Netti, H. C. Lichtenbeld, R. J. Melder and R. K. Jain, *Nat Biotechnol*, 1997, **15**, 778-783.
7. K. R. Levental, H. Yu, L. Kass, J. N. Lakins, M. Egeblad, J. T. Erler, S. F. Fong, K. Csiszar, A. Giaccia, W. Weninger, M. Yamauchi, D. L. Gasser and V. M. Weaver, *Cell*, 2009, **139**, 891-906.
8. F. Montel, M. Delarue, J. Elgeti, L. Malaquin, M. Basan, T. Risler, B. Cabane, D. Vignjevic, J. Prost, G. Cappello and J. F. Joanny, *Physical review letters*, 2011, **107**, 188102.
9. J. M. Tse, G. Cheng, J. A. Tyrrell, S. A. Wilcox-Adelman, Y. Boucher, R. K. Jain and L. L. Munn, *Proc Natl Acad Sci U S A*, 2012, **109**, 911-916.
10. F. Hirschhaeuser, H. Menne, C. Dittfeld, J. West, W. Mueller-Klieser and L. A. Kunz-Schughart, *J Biotechnol*, 2010, **148**, 3-15.
11. J. F. Laurent, C.; Cazales, M.; Mondésert, O.; Ducommun, B. and Lobjois, V., *BMC Cancer*, 2013, **13**.
12. K. Guevorkian, M. J. Colbert, M. Durth, S. Dufour and F. Brochard-Wyart, *Physical review letters*, 2010, **104**, 218101.
13. T. Vasilica Stirbat, S. Tlili, T. Houver, J. P. Rieu, C. Barentin and H. Delanoe-Ayari, *The European physical journal. E, Soft matter*, 2013, **36**, 84.
14. R. Kamm , J. Lammerding and M. Mofrad, Springer Handbook and Nanotechnology, Berlin Heidelberg, 2010, pp. 1171-1196.
15. O. du Roure, A. Saez, A. Buguin, R. H. Austin, P. Chavrier, P. Silberzan and B. Ladoux, *Proc Natl Acad Sci U S A*, 2005, **102**, 2390-2395.
16. A. Ganz, M. Lambert, A. Saez, P. Silberzan, A. Buguin, R. M. Mege and B. Ladoux, *Biol Cell*, 2006, **98**, 721-730.
17. S. Johari, V. Nock, M. M. Alkaisi and W. Wang, *Lab on a chip*, 2013, **13**, 1699-1707.
18. J. L. Tan, J. Tien, D. M. Pirone, D. S. Gray, K. Bhadriraju and C. S. Chen, *Proc Natl Acad Sci U S A*, 2003, **100**, 1484-1489.
19. L. Trichet, J. Le Digabel, R. J. Hawkins, S. R. Vedula, M. Gupta, C. Ribrault, P. Hersen, R. Voituriez and B. Ladoux, *Proc Natl Acad Sci U S A*, 2012, **109**, 6933-6938.
20. F. M. Sasoglu, A. J. Bohl and B. E. Layton, *Journal of Micromechanics and Microengineering*, 2007, **17**, 10.
21. Q. Cheng, Z. Sun, G. A. Meininger and M. Almasri, *Rev Sci Instrum*, 2010, **81**, 106104.
22. P. Roca-Cusachs, F. Rico, E. Martinez, J. Toset, R. Farre and D. Navajas, *Langmuir*, 2005, **21**, 5542-5548.
23. D. Copic, S. J. Park, S. Tawfick, M. F. De Volder and A. J. Hart, *Lab on a chip*, 2011, **11**, 1831-1837.
24. J. S. Kuo, Y. Zhao, L. Ng, G. S. Yen, R. M. Lorenz, D. S. Lim and D. T. Chiu, *Lab on a chip*, 2009, **9**, 1951-1956.
25. H. W. Kuhn, *Naval Research Logistics Quarterly*, 1955, **2**, 83-97.
26. D. Chandra and S. Yang, *Acc Chem Res*, 2010, **43**, 1080-1091.
27. A. Bernard and P. Renault, *Advanced Materials*, 2000, **12**, 1067-1070.
28. C. A. Lemmon, N. J. Sniadecki, S. A. Ruiz, J. L. Tan, L. H. Romer and C. S. Chen, *Mech Chem Biosyst*, 2005, **2**, 1-16.
29. C. Thibault, C. Severac, A. F. Mingotaud, C. Vieu and M. Mauzac, *Langmuir*, 2007, **23**, 10706-10714.
30. D. Fuard, T. T. Chevolleau, S. Decossas, P. Tracqui and P. Schiavone, *Microelectronic Engineering*, 2008, **85**, 1289-1293.
31. S. Raghavan, R. A. Desai, Y. Kwon, M. Mrksich and C. S. Chen, *Langmuir*, 2010, **26**, 17733-17738.
32. Z. Wu, B. Willing, J. Bjerketorp, J. K. Jansson and K. Hjort, *Lab on a chip*, 2009, **9**, 1193-1199.

Lab on a Chip Accepted Manuscript